Reprinted from Preprint Volume, 14th Conference on Severe Local Storms, October 29 - November 1, 1985, Indianapolis, Ind. Published by the American Meteorological Society, Boston, Mass.

2.1

Mesoscale Analysis of Low-Level Temperature and Water Vapor Distribution based on Surface and Satellite Observations

J.F. Weaver, R.M. Zehr and J.F.W. Purdom
NOAA/NESDIS
Regional and Mesoscale Meteorology Branch
Cooperative Institute for Research in the Atmosphere
Colorado State University
Fort Collins, Colorado

1. Introduction

An accurate assessment of low-level temperature and water vapor distribution is important to an accurate weather forecast. It is particularly crucial when forecasting mesoscale events such as deep convection. Classically, this information has been synthesized from a combination of synoptic radiosonde data and from hourly surface observations. However, vertical profiles of temperature and moisture can change appreciably in periods much less than twelve hours (e.g., Fuelberg and Scoggins, 1977). Additionally, the horizontal distribution of both temperature and moisture are typically more detailed than can be resolved by the National Weather Service (NWS) surface observing network. This has been demonstrated by the Program for Regional Observing and Forecast Services (PROFS) field experiments, using a high data density network over northeast Colorado (e.g. Schultz and Schlatter, 1984). The PROFS experiments have also verified that mesoscale forecasts improve with improved data resolution.

In this paper, GOES image and sounding (VAS) data are used in conjunction with conventional observations to study the development of deep convection which produced severe weather and locally heavy rains over the Central Plains on 21-22 June 1984. The major emphasis is on the creation of a very detailed boundary layer analysis to help explain the observed convective development.

2. Data

Conventional upper air and surface data were supplied by the NWS observing network. Visible (VIS) and Infrared (IR) satellite data were collected at special frequencies of 3 to 15 min. Additionally, retrieval information from three hourly VAS observations (averaged to 75 km horizontal resolution) were available. An IBM personal computer (PC) meteorological workstation (Green and Weaver, 1985), allowed display and analysis of the VAS sounding retrievals along with thermodynamic parameters derived from them.

3. 21 June 1984 -- Synoptic Situation

The 1200 GMT surface analysis depicted several features of interest (Fig. 1a). A cold front which had pushed into the western Dakotas to the north, trailed westward through central Wyoming. A stationary front extended southeastward from central South Dakota (SD). Showers and thundershowers were located along this boundary in both eastern SD and eastern Kansas (KS). A lee trough had developed, and extended from western SD to a region of low pressure in southwest KS.

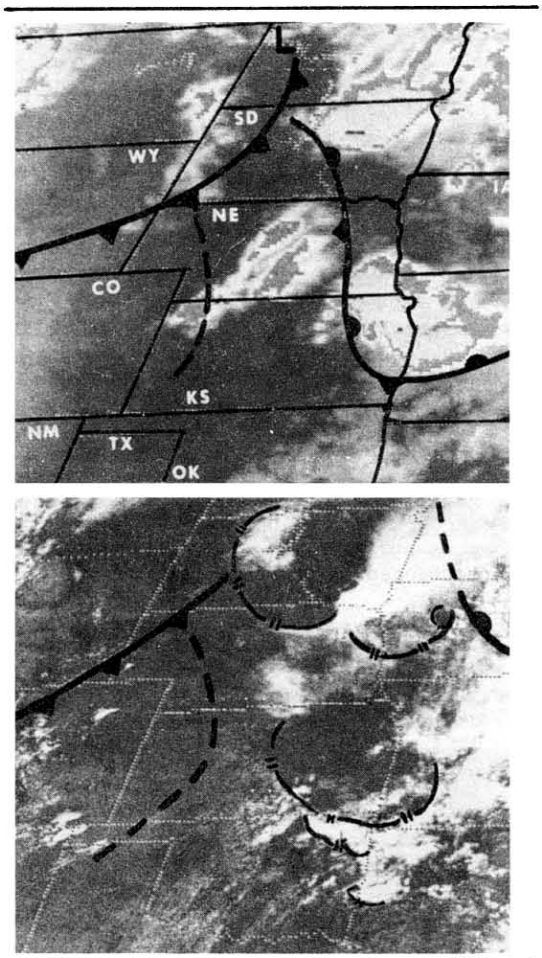

Figure 1. GOES-East satellite imagery from 21 JUN 84 with surface features superimposed (see text). a) 1201 GMT infrared image, b) 1931 GMT VIS image.

At upper levels (not shown), the pattern was generally weak. A subtropical high was building over the Gulf of Mexico. Winds at 500 mb were southwesterly at 20 kts over NE and KS, but further to the south became light and variable. 700 and 850 mb analyses had anticyclonic flow over the entire southcentral plains. 850 mb showed a wind maximum (~35 kts) extending from the Gulf of Mexico into KS. Dewpoints in this windband ranged from 11 °C to 17°C. The forecast for MCS activity (Staff, WRP, 1985) suggested that storms in eastern KS would develop into a large MCS later in the day as the low-level jet intensified in that

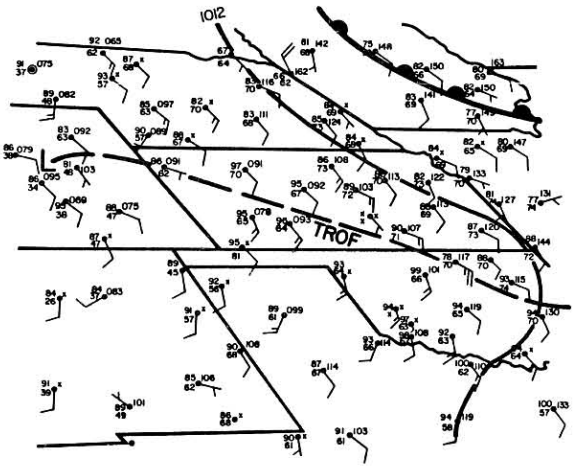

Figure 2. NMC surface analysis for 2100 GMT on 21 JUN 1984 remapped to GOES-West satellite projection.

area (due to the approaching cold front).

By early afternoon, VIS satellite imagery revealed heavy cumulus cloud streets in the unstable air of the 850 mb moist "jet" -- especially in Texas (TX) and Oklahoma (OK) (see Fig. 1b). The stationary front (from 1200 GMT) had moved slowly northeastward as a warm front, but sequential satellite imagery showed that the early thunderstorms had remained behind. As they dissipated, they left a clear, stable air mass which gradually encompassed most of the eastern portion of KS. Similar air masses were found in the eastern Dakotas, extreme northeast NE, and a small region along the western section of the KS/NE border. New thunderstorm activity was forming in northern OK where the low-level moist flow intersected the outflow boundary moving in from KS.

4. Afternoon Development -- Satellite Mesoanalysis

Figure 2 is the NMC surface analysis for 2100 GMT, remapped to a GOES-West projection. Note

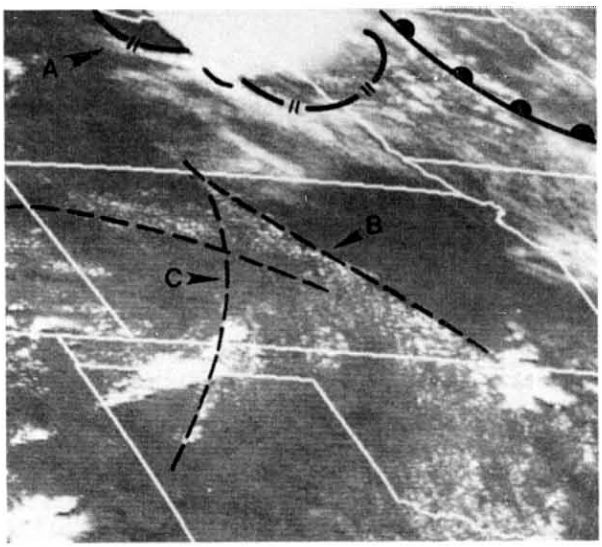

Figure 3. Important low-level airmass features as identified by combined surface/satellite analysis. Surface data 2100 GMT. VIS image from 2045 GMT.

that the only feature shown by the analysis in either KS or NE is an extremely weak pressure trough. Given the unstable airmass (suggested by earlier rawinsonde data), this would be the region to watch for future convective development. However, satellite imagery reveals a much more complex situation.

The VIS image from 2045 GMT (Fig. 3) shows that new storms have formed along the well-developed outflow in NE (A in Fig. 3). Also evident is a clear, and apparently capped, region in eastern KS whose western edge is marked by boundary B. An organized line of cumulus congestus in western KS (C, Fig. 3) corresponds to the extrapolated position of the lee trough described earlier. Evidence in the 2100 conventional data is insufficient to substantiate the connection, however, sequential imagery does establish the relation. Intense convection has developed along this boundary in southwest KS and the OK panhandle. Note also the field of cumulus just north of the trough in northwest KS.

Figure 4 is a temperature analysis for 2100 GMT whose detail has been enhanced utilizing the imagery. The method used takes several factors into account. First, the temperature of the ground is known to be directly related to that of the air in many instances (Geiger, 1966). Furthermore, the 11 μm IR channel constitutes a so-called atmospheric "window", wherein radiation emanating from the ground at that frequency is only minimally absorbed by atmospheric constituents, chief of which is water vapor (e.g., Aoki and Inoue, 1982). Lastly, IR temperature data may be affected small cumulus clouds, since IR data points are at a resolution of ∿7x12 km at the latitude of central KS, and the overall temperature may include sub-pixel cloud influence. The analysis technique currently under study accounts for all of these factors. First, the IR brightnesses are normalized to shelter temperatures in completely clear regions. Next using the CSU interactive processing system (Green and Kruidenier, 1982) VIS imagery is altered to pure white at cloud PIXELS and black at others. The altered image is then degraded to IR resolution, giving a cloud-cover weighting factor which is then applied to the infrared imagery. Finally, surface dewpoint data are used to partition various humidity regimes for individual analysis. In clear regions, or those dominated by small cumulus, the technique shows promise. For regions with a large amount of cloud cover, or mixed cloud types, results are mixed.

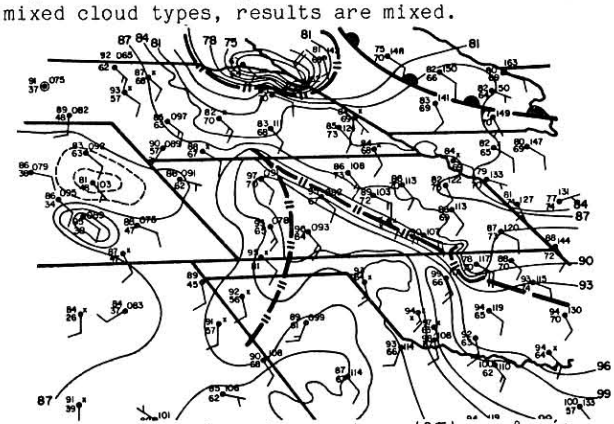

Figure 4. Surface temperature (°F) analysis for 2100 GMT. Boundary locations and some isotherm detail added with satellite assistance (see text).

The temperature analysis provides evidence for most of the mesoscale features identified in the imagery. Cold air pockets are associated with thunderstorm activity in NE, as well as the new storms in northcentral OK. A well-defined temperature gradient is found along boundary B, and clearly demonstrates the airmass discontinuity. Even along boundary C, a slight temperature maximum reinforces the subjective analysis. Note the tongue of very warm temperatures pushing into central KS between boundaries B and C. Perhaps the only feature not substantiated by Figure 4, is the warm front in Iowa (IA).

5. Analysis of VAS Retrievals

VAS retrievals (vertical profiles of temperature and dew point) were obtained from NESDIS Development Laboratory, Madison, Wisconsin. The retrieval algorithm is described by Smith and Woolf (1984). Between 70 and 115 retrievals at 75 km resolution were available every 3 hours over the Central Plains between 1118 GMT, 21 June and 0518 GMT, 22 June. These data were analyzed on the IBM-PC workstation. PC analysis routines included software for displaying vertical soundings, horizontal fields of retrieval variables, and derived thermodynamic parameters. Tabular listings of retrieval variables and derived parameters included such data as lowest km mixing ratio, height of the lifting condensation level (LCL) and convective condensation level (CCL), convective temperature, positive buoyant energy using either the LCL or CCL, low-level negative buoyancy, and many others. Analysis of VAS-derived thermodynamic energy parameters have proven very useful in defining mesoscale air mass characteristics.

Comparisons of temperature lapse rates and vertical water vapor profiles agree with the air mass differences discussed in Section 4. Sets of adjacent retrievals with very small differences were grouped together to define specific air masses, with both upper and lower tropospheric characteristics being used in the interpretation. The subsets of similar retrievals were compared to define air mass and boundary characteristics. The results, illustrated in Figure 5, are blocky due to the 75 km resolution of the data. Characteristics of each of the air masses are briefly summarized in Table 1.

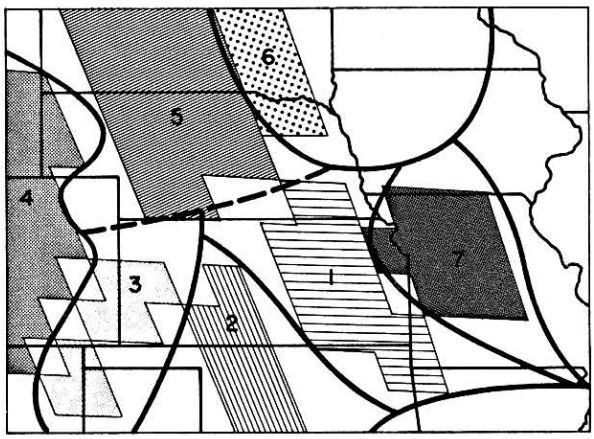

Figure 5. Various airmasses at 2318 GMT as defined by VAS retrieval data. The boundaries were located with VISSR and conventional data. Dashed lines indicate upper- and solid lines indicate lower-tropospheric boundaries.

Table 1: Mesoscale Air Mass Characteristics

#*	Air Mass Characteristic	T_{sfc}(°F)	T_{dsfc}(°F)	B_{VAS} (Jkg^{-1})
1	capped, very moist	83-88	70-75	2316
2	hot, moist	93-97	62-67	1829
3	hot, less moist	88-97	48-63	1250
4	very warm, dry	82-92	35-48	989
5	warm, moist	83-92	62-70	2578
6	rain cooled, subsidence	65-81	62-68	1738
7	cool, very moist	78-82	68-72	1145

*For region #'s refer to Figure 5.

The sub-cloud layer distribution of water vapor is crucial to the evolution of mesoscale convective systems. The contribution of VAS low-level moisture information is illustrated in Figure 6. Figure 6a is the dewpoint analysis based on surface observing stations, while the VAS retrieval-derived average dewpoint in the surface to one kilometer layer is shown in Figure 6b. Note the detail added to the analysis by the VAS radiances via the retrieval algorithm. There is often more detail in the dewpoints analyzed from surface stations (Fig. 6a), than can be provided by VAS retrievals, and we note that retrievals derived from more detailed surface data as a "first guess" might result in better low-level water vapor fields. Nevertheless, VAS low-level moisture fields are very important since they provide layer averaged moisture not available from

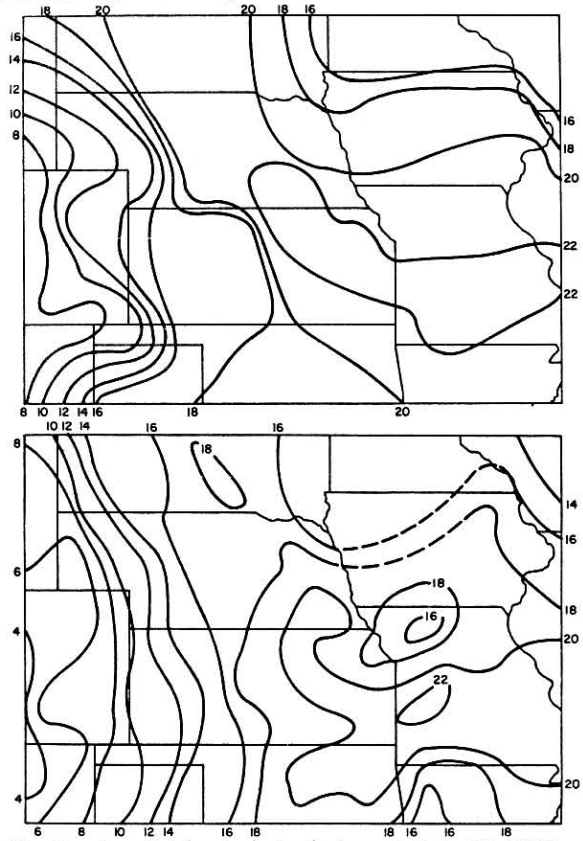

Figure 6. Various dewpoint analyses at 0000 GMT, 22 June 1984. Analyses are a) based on surface observations, and b) integrate lowest kilometer dewpoints from VAS retrievals.

surface observations, as well as space and time resolution not available in the conventional rawinsonde network.

The average available buoyant energy from the VAS retrievals (B_{VAS}) is given in Table 1 for each air mass. These values were computed by adiabatically lifting a parcel mixed in the lowest kilometer. Air mass 1 is referred to in Section 4 as "a clear and apparently capped region". VAS shows this air mass is indeed relatively cool at the surface compared to air masses 2, 3, 4 and 5. The term "capped" in Table 1, refers to a stable layer found near the top of the boundary layer. This feature was revealed both in the VAS retrievals and in 0000 GMT radiosonde observations at Topeka, KS and Monett, MO. Thus, despite the high buoyant energy (2316 Jkg^{-1}), air mass 1 was not favorable for deep convection, without strong lift or heating. Similarly, air masses 6 and 7 have substantial positive area, but require large heating or lift for convection. Note that air mass 5 has higher available buoyant energy than air mass 2 (Table 1) despite cooler surface temperature and comparable dewpoints. This is because of a cooler mid- to upper-troposphere in air mass 5 (Figure 5) to the north of the Kansas-Nebraska border.

Various computed parameters from the VAS sounding analyses confirm the low-level analysis of Section 4. Fields of positive buoyant energy, negative buoyancy (surface-LCL), negative buoyancy (LCL-LFC), and "energy necessary to reach convective temperature" were of particular interest. Strongly capped regions were associated with air masses 1, 6 and 7, while high positive buoyancy was associated with air masses 1, 2 and 5.

At approximately 2200 GMT, a thunderstorm formed at the intersection of boundaries B and C (Fig. 3) separating air mass 1 and 2 (Fig. 5). The storm grew rapidly in both size and intensity as it tracked slowly southeastward along boundary B. The storm fostered a small tornado and brought several reports of large hail including one of baseball size. Strong winds and heavy rain were also common. As the evening progressed, the activity expanded to become a meso-β scale MCS which lasted into the nighttime hours.

In other parts of the region, a large mesoscale system developed in western Montana and the western Dakotas feeding on air mass 5. The convection with the outflow spreading southward across Iowa dissipated as it moved into the unfavorable region dominated by air mass 7.

6. Summary and Concluding Remarks

The main objective in presenting the foregoing analysis was to discuss ways to better define the low-level, three-dimensional state of the atmosphere with as much detail as possible ... using all of the data sources at hand. In the case presented, it was shown how satellite image and sounding data could be used to provide much of this detail.

The discussion began with a conventional surface analysis (Fig. 2), to which substantial information was immediately added via VIS imagery (Fig. 3). The temperature field was analyzed, then enhanced using IR data as described in Section 4 (Fig. 4). Finally, several different air masses were identified using VAS retrieval data (Fig. 5). By combining the information from both Figure 4 and 5, it is clear that even more air mass information is available (than that from VAS alone). For example, a wedge of cooler temperatures extends from southeast New Mexico into northwest OK. This would have been important forecast input when storms which formed along boundary C in the TX and OK panhandles, later began moving into northwest OK. An awareness of this cool wedge might temper the forecast severity of that activity considerably. By the same token, the exceptionally hot temperatures along boundary B, might suggest a greater chance for activity becoming more severe there.

The thermodynamic energy parameters in Section 5 are vertically integrated quantities. VAS retrievals are particularly suited for this type of computation, since they are, by their nature, layer-averaged observations. The buoyant energy computations utilize temperature, dewpoint and pressure of the lifting parcel, as well as cloud layer, environmental lapse rates. Of these, the lapse rate and parcel dewpoint are the strongest factors in parcel buoyancies. However, the buoyant energy available to a convective cloud is a result of a mixed boundary layer value. That is why surface dewpoint data alone can be misleading -- moist air might be confined to a very shallow layer, with very dry air just above. For this reason, low-level water vapor fields derived from VAS sounding data may represent the sub-cloud layer more reasonably.

8. Acknowledgements

Research support was provided for this work through NOAA Grants NA84AA-D-00017 and NA84AA-H-00020. We would like to thank Sallie Varner for her work in the preparation of the text.

9. References

Aoki, T. and T. Inoue, 1982: Estimation of the precipitable water from the IR channel of the geostationary satellite. Remote Sens. of the Env., 12, 219-228.

Fuelberg, H.E. and J. Scoggins, 1977: Relationship between the kinetic energy budget and intensity of convection. Proc. 10th Conf. on Severe Local Storms, Omaha, Amer. Meteor. Soc., 265-270.

Geiger, R., 1966: The Climate Near the Ground. Harvard Univ. Press, 79 Garden St., Cambridge, MA 02138, 611 pp.

Green, R.N. and M. Kruidenier, 1982: Interactive data processing for mesoscale forecasting applications. Proc. 9th Conf. on Wea. Forecasting and Anal., Amer. Meteor. Soc., 60-64.

Green, R.N. and J.F. Weaver, 1985: Use of a personal computer workstation for short range forecasting: A case study. Proc. 14th Conf. on Severe Local Storms, Indianapolis, Amer. Meteor. Soc. (this volume).

Schultz, P. and T.W. Schlatter, 1984: Forecasting high plains convection with the PROFS system. Preprints, 10th Conf. on Wea. Forecasting and Anal., 25-29 June, Clearwater, FL, Amer. Meteor. Soc., 480-485.

Smith, W.L. and H. Woolf, 1984: Improved vertical soundings from an amalgamation of polar and geostationary radiance observations. Preprints, Conf. on Sat. Remote Sens. and Appl., 25-29 June, Clearwater, Amer. Meteor. Soc., 45-48.

Staff, Weather Research Program, 1985: 1984 Airborne Investigations of Mesoscale Convective Systems (AIMCS): Operational summary and data inventory. NOAA Tech Memo ERL ESG-9, Envir. Sci. Group, NOAA/ERL, Boulder, CO 80303, 74 pp.